Cellular/Molecular

C-Jun N-Terminal Kinase Post-Translational Regulation of Pain-Related Acid-Sensing Ion Channels 1b and 3

Clément Verkest, Sylvie Diochot, Eric Lingueglia, and ⬤Anne Baron

Université Côte d'Azur, Centre National de la Recherche Scientifique, Institut de Pharmacologie Moléculaire et Cellulaire Laboratoire d'Excellence Canaux Ioniques d'Intérêt Thérapeutique, Fédération Hospitalo-Universitaire InovPain, 06000 Nice, France

Neuronal proton-gated acid-sensing ion channels (ASICs) participate in the detection of tissue acidosis, a phenomenon often encountered in painful pathologic diseases. Such conditions often involve in parallel the activation of various signaling pathways such as mitogen activated protein kinases (MAPKs) that ultimately leads to phenotype modifications of sensory neurons. Here, we identify one member of the MAPKs, c-Jun N-terminal kinase (JNK), as a new post-translational positive regulator of ASICs in rodent sensory neurons. Recombinant H^+-induced ASIC currents in HEK293 cells are potently inhibited within minutes by the JNK inhibitor SP600125 in a subunit-dependent manner, targeting both rodent and human ASIC1b and ASIC3 subunits (except mouse ASIC3). The regulation by JNK of recombinant ASIC1b- and ASIC3-containing channels (homomers and heteromers) is lost on mutation of a putative phosphorylation site within the intracellular N- and the C-terminal domain of the ASIC1b and ASIC3 subunit, respectively. Moreover, short-term JNK activation regulates the activity of native ASIC1b- and ASIC3-containing channels in rodent sensory neurons and is involved in the rapid potentiation of ASIC activity by the proinflammatory cytokine TNFα. Local JNK activation *in vivo* in mice induces a short-term potentiation of the acid-induced cutaneous pain in inflammatory conditions that is partially blocked by the ASIC1-specific inhibitor mambalgin-1. Collectively, our data identify pain-related channels as novel physiological JNK substrates in nociceptive neurons and propose JNK-dependent phosphorylation as a fast post-translational mechanism of regulation of sensory-neuron-expressed ASIC1b- and ASIC3-containing channels that may contribute to peripheral sensitization and pain hypersensitivity.

Key words: ASICs; DRG neuron; inflammation; JNK; pain; TNF-alpha; sodium channel

---

Significance Statement

ASICs are a class of excitatory cation channels critical for the detection of tissue acidosis, which is a hallmark of several painful diseases. Previous work in sensory neurons has shown that ASICs containing the ASIC3 or the ASIC1b subunit are important players in different pain models. We combine here functional and pharmacological *in vitro* and *in vivo* approaches to demonstrate that the MAP Kinase JNK is a potent post-translational positive regulator, probably *via* direct phosphorylation, of rodent and human ASIC1b- and ASIC3-containing channels. This JNK-dependent, fast post-translational mechanism of regulation of sensory-neuron-expressed ASICs may contribute to peripheral sensitization and pain hypersensitivity. These data also identify pain-related channels as direct downstream effectors of JNK in nociceptors.

Introduction

Chemodetection of noxious and innocuous stimuli by sensory neurons encompasses the detection of a broad range of chemically distinct molecules such as protons, lipids, irritants, toxins, or cytokines, often encountered in inflammatory or itch processes (Petho and Reeh, 2012). The various pain-related mediators that are released act on receptors and associated signaling pathways, which are critical in the establishment of pain hypersensitivity (Hucho and Levine, 2007). Such signaling pathways include several protein kinases like protein kinase A (PKA) or protein kinase C (PKC) and also several members of the mitogen-activated protein kinase (MAPK) family like extracellular signal-regulated kinase, p38, and c-jun N-terminal kinase (JNK; Obata et al., 2004). JNK is of particular interest regarding its

activation in DRG neurons, which has been well established in various pain models including migraine (Huang et al., 2016), neuropathic, and cancer pain (Simonetti et al., 2014).

Acid-sensing ion channels (ASICs) are critical for the detection of tissue acidosis, which is a hallmark of several painful diseases (Dinkel et al., 2012; Deval and Lingueglia, 2015). At least six subunits are expressed in rodents (ASIC1a, ASIC1b, ASIC2a, ASIC2b, ASIC3, and ASIC4), encoded by four genes, which associate into trimeric functional channels that are widely distributed in the nervous system and all along the pain pathway. In addition to protons, ASICs can be modulated by multiple pain-related mediators, including lipids (Smith et al., 2007; Marra et al., 2016), small molecules (Cadiou et al., 2007; Li et al., 2010), and neuropeptides (Askwith et al., 2000). Early work on ASICs in sensory neurons has shown that the ASIC3 subunit is an important player in different pain models (Deval et al., 2008; Yan et al., 2013; Marra et al., 2016). Recent pharmacological and genetic evidence have refined this idea by proposing that ASIC1-, and especially sensory-neuron-specific ASIC1b-containing channels, can also participate in peripheral pain (Bohlen et al., 2011; Diochot et al., 2012, 2016; Verkest et al., 2018; Chang et al., 2019).

We combine here functional and pharmacological *in vitro* and *in vivo* approaches to demonstrate that the MAPK JNK is a potent post-translational regulator of ASIC1b and ASIC3. JNK activation potentiates within minutes the activity of recombinant and native ASIC1b- and ASIC3-containing channels in a species-dependent manner. The effect is dependent on key residues in a putative phosphorylation site within the N-terminal domain of rat, mouse, and human ASIC1b, and the C-terminal domain of rat and human, but not mouse, ASIC3. Local activation of JNK *in vivo* in mice evokes a short-term and partially ASIC1-dependent potentiation of the acid-induced cutaneous pain in inflammatory conditions.

Materials and Methods

Animals. Experiments were performed on male C57BL/6J mice 6–14 weeks old, weighing 20–25 g, and 6- to 8-week-old male Wistar rats (Charles River Laboratories). Animals were housed in a 12 h light/dark cycle with food and water *ad libitum* and were acclimated for at least 1 week before being subjected to experiments. Animal procedures were approved by the government's local ethics committee and authorized by the French Ministry of Research according to European Union regulations and Directive 2010/63/EU (Agreements E061525 and APAFIS#20 260-2019040816489112). Animals were killed at experimental end points by CO_2.

Chemicals. For stock solutions, the MAPK activator anisomycin (Tocris Bioscience), the JNK inhibitor SP600125 (Selleckchem), and the transient receptor potential vanilloid 1 (TRPV1) inhibitor capsazepine (Sigma) were dissolved in DMSO, and TNFα (PeproTech) in saline solution (NaCl 0.9%). Final dilution was made just before the experiments. The final concentration of DMSO never exceeded 0.1% including in the control extracellular solution and during patch-clamp experiments and never exceeded 0.5% including in the vehicle saline solution and during *in vivo* behavior experiments. ASIC-targeting toxins psalmotoxin-1 (PcTx1), APETx2, and mambalgin-1 (Mamb) that were shown to block ASIC1a (Escoubas et al., 2000), ASIC3-containing channels (Diochot et al., 2004), and both ASIC1a- and ASIC1b-containing channels (i.e., ASIC1-containing channels; Diochot et al., 2012), respectively, were purchased from Smartox and dissolved in water or saline, with 0.05% bovine serum albumin (BSA; 99% fatty acid free, Sigma) added to the final solution for patch-clamp or behavior experiments to avoid nonspecific adsorption on vessels and tubings.

Mutagenesis and site prediction analysis. Point mutants were obtained by recombinant PCR strategies as previously described (Salinas

et al., 2009) using the following primers: rat ASIC1b S59A, forward: 5′-AGGGTGATGACGCACCTAGGGAC-3′, reverse: 5′-GTCCCTAGGT GCGTCATCACCCT-3′, mouse ASIC3 A509T, forward: 5′-CC TCCTACCACTCCCAGTGCT-3′, reverse: 5′-AGCACTGGGAGT GGTAGGAGG-3′. Constructs were subsequently subcloned into pIRES2-EGFP vector using NheI-EcoRI restriction enzymes. All constructs were fully sequenced to confirm the presence of the desired mutation.

Site prediction analysis was carried on intracellular N-terminal and C-terminal sequences of ASIC1a, 1b, 2a, 2b, from three different species (mouse, rat, and human, UniProt) using eukaryotic linear motif (ELM) resource (Dinkel et al., 2012). Subsequent analysis for putative phosphorylation sites was run using Group-Based Prediction System (GPS) software (version 5.0; Xue et al., 2008) with a medium sensitivity threshold to refine the list of potential protein kinases.

Cell culture. HEK293 cells were grown in DMEM medium (Lonza) with 10% fetal bovine serum (Biowest) and 1% Penicillin/Streptomycin (Lonza) in an incubator at 37°C with 5% CO_2. One day after being plated at a density of 20,000 cells in 35 mm diameter dishes, cells were transfected with one or several of the following plasmids: pIRES2-rASIC1a-EGFP, pCI-rASIC1a, pIRES2-rASIC1b-EGFP, pCI-rASIC1b, pCI-rASIC2a, pIRES2-rASIC2b-EGFP, pCI-rASIC2b, pIRES2-rASIC3-EGFP, pCI-rASIC3, pIRES2-EGFP, pIRES2-hASIC1b-EGFP, pIRES2-hASIC3a-EGFP, or pIRES2-hASIC1a-EGFP vectors using the JetPEI reagent according to the supplier's protocol (Polyplus Transfection). Generally, 0.5 µg of DNA per dish was used, except 1 µg for homomeric ASIC3. For coexpression of two ASIC subunits, a 1:1 plasmid ratio was used. Fluorescent cells were selected for patch-clamp recordings 2–4 d after transfection. Heteromeric currents were identified by combining several biophysical and pharmacological properties.

DRG neurons were prepared from male C57Bl6J mice (6–14 weeks old) and Wistar male rats (6-8 weeks old) and processed in a similar way, unless mentioned otherwise, than previously described (Francois et al., 2013). After isoflurane anesthesia, rats and mice were killed by decapitation and thoracolumbar DRGs were collected on cold HBSS and enzymatically digested at 37°C for 40 min with collagenase II (2 mg/ml, 235 U/mg, Biochrom) for mice, collagenase I (4 mg/ml, 370 U/mg, Worthington) for rats, and dispase II (5 mg/ml, 1.76 U/mg, Invitrogen) for both. Gentle mechanical dissociation was performed with a 1 ml syringe and several needles with progressively decreasing diameter tips (18, 21, and 26 ga) to obtain a single-cell suspension. Neurons were plated on poly-D-lysine/laminin coated dishes with the following media: Neurobasal-A (Invitrogen) completed with L-glutamine (2 mM final, Lonza), B27 supplement (1×, Invitrogen) and 1% Penicillin/Streptomycin. One to 2 h later, neurons were carefully washed to remove cellular debris and incubated with complete medium. The following additional growth factors were used: nerve growth factor (NGF) 100 ng/ml and retinoic acid, 100 nM (Sigma); glial derived neurotrophic factor (GDNF), 2 ng/ml; and brain derived neurotrophic factor (BDNF), 10 ng/ml, and Neurotrophin 3, 10 ng/ml (PeproTech). Patch-clamp recordings were done 1–4 day after plating on both small (membrane capacitance <40 pF) and large (>40 pF) diameter neurons. Acutely dissociated mouse DRG neurons were processed the same way as above, except they were incubated without the additional neurotrophic growth factors listed above to limit basal activation of JNK and permit observation of activating effects. They were recorded 3–10 h after plating.

Patch-clamp recording experiments. Ion currents were recorded using the whole-cell patch-clamp technique. Recordings were made at room temperature using Axopatch 700A or Axopatch 200B (Molecular Devices) amplifiers, with a 2–5 kHz low-pass filter. Data were sampled at 10 kHz using pClamp9 or pClamp10 software. The borosilicate patch pipettes (2–7 MΩ) contained the following (in mM): 135 KCl, 5 NaCl, 2 $MgCl_2$, 2 $CaCl_2$, 5 EGTA, and 10 HEPES (pH 7.25 with KOH). To investigate regulations by mediators or protein kinases in HEK293 cells and DRG neurons, 2.5 mM Na_2-ATP was used instead of NaCl. The control bath solution contained the following (in mM): 145 NaCl, 5 KCl, 2 $MgCl_2$, 2 $CaCl_2$, 10 glucose, and 10 HEPES (pH 7.4 with NaOH). MES was used instead of HEPES to buffer solutions with a pH ≤6. Cells were

Table 1. Pharmacological evidence supporting the proposed association between toxin inhibition profiles and ASIC channel subtypes

Toxin inhibition profiles (i.e., currents only inhibited by the indicated toxins among the three tested)	Possibly associated ASIC channel subtypes (Toxin selectivity)		
	ASIC1a (PcTx1 or Mamb-1)	ASIC1a/2a or **ASIC1b-containing** (Mamb-1)	**ASIC3-containing** (APETx2)
Mamb-1 + APETx2 + PcTx1	Yes	Yes	Yes
Mamb-1 + APETx2	No	Yes	Yes
Mamb-1 + PcTx1	Yes	Yes	No
Mamb-1	No	Yes	No
APETx2	No	No	Yes

ASIC channel subtypes possibly associated (Yes) or not (No) with the different pharmacological profiles determined by testing the inhibitory effects of mambalgin-1 (1 μM), APETx2 (3 μM) and PcTx1 (20 nM). Channel subtypes regulated by JNK in vitro are indicated in bold. Only ASIC1b-containing channels are regulated in mice, including heteromeric channels with ASIC3. Note that when different pharmacologically distinct types of channels are present together into a neuron (e.g., ASIC1b-containing and ASIC3-containing channels), the proportion of each channel type can significantly vary depending on the percentage of inhibition induced by each toxin, which can vary from 20% (threshold for inhibition) to 100%.

voltage clamped at a holding potential of −60 mV (HEK293) or at −80 mV for neurons (i.e., close to the K$^+$ equilibrium potential to minimize K$^+$ current contribution). ASIC currents were activated by a rapid pH drop by shifting one of eight outlets of a gravity-driven perfusion system from a control solution (i.e., pH 7.4 or pH 8.0) to an acidic test solution. To test the effect of a mediator or a signaling pathway, ASIC currents were repetitively activated every 30 s for the ASIC1b homomeric current, every 15 s for the ASIC3 homomeric current, and every minute for the ASIC1a homomeric current (these intervals allowing full reactivation). Drugs were perfused for at least 5 min and up to 10 min in the pH 7.4 control bath solution until maximal effect was observed. Activation curves were determined by activating whole-cell ASIC currents at a given pH after a 30 s perfusion of control pH 8.0 solution. Inactivation curves were obtained by maximally activating whole-cell ASIC currents by pH 5.0, pH 4.5 or pH 4.0 after a 30 s perfusion at a given pH. The curves of pH-dependent activation and inactivation were fitted by a Hill function: $I = a + [(I_{max} − a)/(1 + (pH_{0.5}/[H]n)]$, where I_{max} is the maximal current, a is the residual current, $pH_{0.5}$ is the pH at which half-maximal activation/inhibition of the transient peak ASIC current was achieved, and n is the Hill coefficient. Time constant of current decay was fitted with a single exponential function.

Outside-out configuration was achieved after whole-cell configuration by slowly pulling out the patch pipette. Intracellular and extracellular media were the same as above. Cells were then perfused with SP600125 for 5 min in the pH 7.4 bath solution, and a drop to pH 5.0 was used to open ASICs.

For DRG neurons, action potentials were evoked in current-clamp mode by 2 ms depolarizing current injections of increasing amplitudes (Δ50 or 100 pA), and neurons that displayed a resting membrane potential superior to −40 mV and/or no action potential were discarded. The time derivative of membrane voltage was calculated to determine whether the falling phase had one or two components (a feature of nociceptive neurons (Petruska et al., 2000)). In voltage-clamp mode, the pharmacological characterization of the ASIC-like peak current was done by applying for 30 s the ASIC inhibitory toxins APETx2 (3 μM), PcTx1 (20 nM), and mambalgin-1 (1 μM), before the pH drop from the resting pH 7.4 to pH 5.0. Toxin experiments were usually performed with activation of the current from the resting pH 7.4 to pH 5.0. An activating pH of 6.6 (from resting pH 7.4) was additionally tested when necessary to improve the functional characterization of the ASIC current. Current was considered sensitive to a toxin if at least 20% of inhibition was observed (Table 1). Investigation of the effect of a signaling pathway was then carried out as described previously on HEK293 cells. In the analysis, 154 mouse DRG neurons from 10 cultures, 49 rat DRG neurons from four cultures, and 28 acutely dissociated mouse DRG neurons from four cultures were used.

In vivo *behavior experiments.* Acid-induced cutaneous pain was evoked in mice by intraplantar (i.pl.), subcutaneous injection (20 μl, 30 ga needle) in the left hindpaw of a pH 5.0-buffered solution (NaCl 0.9%, MES 20 mM, pH 5.0 with NaOH). To test the local pharmacological effect, drugs were preinjected 10 min before (10 μl, 30 ga needle) in a nonbuffered saline solution (NaCl 0.9%) to allow diffusion within the

tissue, then coinjected with the pH 5.0 solution. Anisomycin and SP600125 were tested at 500 μM (a higher concentration than the one used in patch-clamp experiments to account for in vivo/in vitro differences), capsazepine was tested at 10 μM (Kwak et al., 1998), mambalgin-1 was tested at 34 μM as previously described (Diochot et al., 2012, 2016), and APETx2 was tested at 10 μM (Deval et al., 2008). The final concentrations of DMSO and BSA were 0.5% (anisomycin, SP600125, anisomycin + SP600125, anisomycin + capsazepine, vehicle) and 0.05% (mambalgin-1 and mambalgin-1 + APETx2-containing solutions and related vehicle), respectively.

Mice were placed in mirror boxes where they acclimated for at least 15 min before undergoing a single pH 5.0 i.pl. injection or the double intraplantar injection protocol (preinjection followed by coinjection) for pharmacological experiments. Duration of spontaneous pain-related behavior (paw licking, shaking, and lifting) was measured over 5 min intervals during 15 min after the pH 5.0 i.pl. injection or from the preinjection 10 min before in the double intraplantar injection protocol.

Paw inflammation was induced by injection of a 2% carrageenan solution (NaCl 0.9%) in the left hindpaw (20 μl, 25 ga) 3 h before measuring the acid-induced cutaneous pain. Mice that did not show a visible red edema (6 of 174) and mice that showed >15 s left hindpaw movements during the 10 min period before the pH 5.0 injection (20 of 169) were excluded to avoid nonpainful behavior (e.g., grooming) or spontaneous pain from other causes (e.g., wounds).

Data statistical analysis. For patch-clamp experiments, data are presented as mean ± SEM along with the individual data points (number of recorded cells indicated in figure legends). Data from the same cell before and after treatment were analyzed by a paired t test or a Wilcoxon nonparametric paired test, and two different groups were compared by an unpaired t test or a Mann–Whitney nonparametric unpaired test. For multiple comparisons, a one-way ANOVA with Tukey's *post hoc* test for multiple comparisons was performed, and $p < 0.05$ was considered statistically significant.

For behavioral experiments, data are presented as mean ± SEM as a function of time (the number of mice are provided in figure legends). Data from the same mice were analyzed by a two-way ANOVA followed by Dunnett's *post hoc* paired comparison with data obtained during the 5 min interval preceding the second intraplantar injection. Data from different mice were compared by a two-way ANOVA followed by Dunnett's *post hoc* unpaired comparison with the data obtained when the second pH 5.0 i.pl. injection was made in the presence of anisomycin; $p < 0.05$ was considered statistically significant (p values and statistical results are provided in figure legends). Analysis in both patch-clamp and behavioral experiments was performed using GraphPad Prism version 4.0 and version 6.0.

Results

Recombinant ASIC1b- and ASIC3-containing channels are positively regulated by short-term JNK activation
Activation of the MAPK JNK has been shown to play an important role in pain, and we investigated the effect of short-term JNK activation on ASIC currents expressed in HEK293 cells

transiently transfected with recombinant ASIC subunits. At the holding potential of −60 mV, a rapid drop of the extracellular pH from 7.4 to 5.0 evoked the rat ASIC1b (rASIC1b) transient inward current (Fig. 1A). When the cells were incubated several minutes with the MAPK activator anisomycin (10 μM) a small increase in the rASIC1b peak current amplitude was sometimes observed but not significantly different from the control current (Fig. 1B). Subsequent incubation with the JNK inhibitor SP600125 (10 μM) for several minutes induced a strong decrease of the rASIC1b current amplitude (Fig. 1A) below the control amplitude, which was consistent with inhibition of a high basal level of JNK activity, which explains the lack of a significant mean stimulatory effect of anisomycin. A potential nonspecific inhibitory effect of SP600125 through direct interaction with the channel was ruled out as the drug had no effect on the rASIC1b current amplitude in outside-out patches ($n = 3$; data not shown). To estimate the JNK total effect on the current, we calculated the ratio of rASIC1b peak current amplitude between the maximally JNK-stimulated (i.e., after anisomycin) and the maximally JNK-inhibited (i.e., after SP600125) currents. JNK increased the rASIC1b current amplitude by ~50% for every test pH used (+63.2 ± 11.6% at pH 6.3, $p < 0.0001$, +48.4 ± 7.9% at pH 6.0, $p = 0.0006$, and +48.0 ± 10.9% at pH 5.0, $p = 0.0009$; Fig. 1B, dark blue bars). JNK regulation did not change the biophysical properties of rASIC1b, with similar $pH_{0.5}$ values for pH-dependent activation (6.08 ± 0.70 after anisomycin vs 6.05 ± 0.09 after SP600125) as well as pH-dependent inactivation (6.78 ± 0.04 after anisomycin vs 6.80 ± 0.04 after SP600125; Fig. 2A) and also similar inactivation time constants (Fig. 2B).

We next explored the effect of JNK in the same conditions on the other homomeric ASIC isoforms except ASIC2b and ASIC4, which are not forming proton-activated channels per se (Baron et al., 2013). The amplitude of the peak current flowing through rat ASIC3 (rASIC3) homomeric channels was also significantly increased (+63.4 ± 23.1% at pH 7.0, $p = 0.015$, and +88.0 ± 25.0% at pH 6.6, $p = 0.015$; Fig. 1C). On the other hand, currents recorded from rat ASIC1a and ASIC2a (rASIC1a and rASIC2a) homomeric channels were not potentiated for every test pH used (Fig. 1D,E). We next tested the effect of JNK on several ASIC heteromers. JNK potentiated the peak current of all the rat ASIC1b- or ASIC3-containing heteromeric channels tested, but not of the rat ASIC1a + 2a channels (Fig. 1F). The sustained currents associated with ASIC3 (Salinas et al., 2009), that is, the window current activated by a pH close to 7.4, as well as the pH 5.0 evoked sustained current, were also potentiated by JNK (+53.4 ± 13.5% for rASIC3 at pH 7.0, $p = 0.0156$, and +27.4 ± 6.1% for rASIC3 + 2b at pH 5.0, $p = 0.0313$; Fig. 1G). The currents flowing through human ASIC1b and ASIC3 channel isoforms were potentiated by JNK in a similar way to that of their rat counterparts (Fig. 3A,B).

These data show that short-term JNK activation exerts a positive regulation of the activity of recombinant rat and human ASIC1b- and ASIC3-containing channels and that the presence of these subunits is necessary and sufficient to confer regulation to heteromeric channels combining subunits that are not regulated, like ASIC1a and ASIC2a.

The JNK regulation is species dependent and depends on a putative phosphorylation site within the intracellular domains of ASIC1b and ASIC3 subunits

To address the mechanism underlying the JNK-dependent potentiation of ASICs, we first performed a bioinformatic

analysis on the intracellular segments of rASICs to identify putative phosphorylation sites. Interestingly, we identified a putative JNK2 phosphorylation site in the rASIC1b N-terminal domain (S59) as well as in the rASIC3 C-terminal domain (T512). These sites are conserved in rat, mouse, and human except for mouse ASIC3 where the threonine is replaced by an alanine (Fig. 4A).

We next performed point mutations of the putative phosphorylation sites to test possible involvement in the effects observed. The rASIC1b S59A mutant had biophysical properties similar to the wild-type channel ($pH_{0.5}$ for activation and inactivation, inactivation time constant; data not shown), but lost the regulation by JNK for every test pH used (Fig. 4B, light blue bars). Consistent with the lack of putative JNK phosphorylation site (Fig. 4A), the mouse ASIC3 channel failed to be potentiated by JNK (Fig. 4C, red bars), but the mASIC3 A509T mutant in which the alanine is replaced by a threonine to create a putative JNK phosphorylation site, was significantly potentiated by the kinase (Fig. 4C, orange bars). Interestingly, because mouse and rat ASIC3 have >96% protein identity, mASIC3 A509 could be indeed considered a natural mutation of the rat ASIC3. Together with the A509T mutation that recreates in mice the rat putative JNK phosphorylation site, this confirms the importance of this phosphorylation site in the JNK-dependent regulation of rat ASIC3.

These results suggest that potentiation of the ASIC1b- and ASIC3-containing channel activity by JNK is supported by a phosphorylation of the ASIC1b and ASIC3 subunits at intracellular S59 and T512, respectively. The importance of this later site is further confirmed by the fact that a single mutation of the putative phosphorylation residue is sufficient to confer JNK-regulation to mouse ASIC3 that is naturally insensitive.

Native ASICs in DRG neurons are positively regulated by short-term JNK activation

The effects of JNK on native proton-gated currents in cultured DRG sensory neurons were then investigated. Rapid extracellular acidification from pH 7.4 to pH 5.0 on randomly selected cultured mouse and rat DRG neurons hold at −80 mV, produced inward currents in all the neurons tested ($n = 101$ and 49, respectively), with various shapes and kinetics. No difference was observed in the average capacitance and resting membrane potential between neurons recorded from rats and mice (see Table 3). Action potential duration and rheobase were, however, different (see Table 3), likely linked to subtle changes in the voltage-gated ion channels profile and distribution. Higher values of ASIC transient current density and peak current inactivation time constant were observed in rat neurons, in agreement with previous data (Leffler et al., 2006). Neurons expressing transient ASIC-like currents, associated or not with a sustained current of variable amplitude, were selected, whereas neurons showing only a sustained current without any peak were excluded. DRG neurons expressed a number of different, and often heteromeric, ASIC channels (Benson et al., 2002; Papalampropoulou-Tsiridou et al., 2020). We used a set of specific and potent ASIC-blocking toxins (Baron et al., 2013) to perform a pharmacological profiling of ASIC-like transient currents recorded in cultured DRG neurons to confirm the channel subtypes possibly associated (PcTx1, APETx2, and mambalgin-1 to block ASIC1a, ASIC3-containing channels, and both ASIC1a- and ASIC1b-containing channels, respectively; Table 1). An inhibition by at least 20% of the ASIC-like peak current by APETx2 (3 μM), PcTx1 (20 nM), or mambalgin-1 (1 μM) was interpreted as a significant participation of ASIC3-containing channels, ASIC1a channels, or ASIC1-
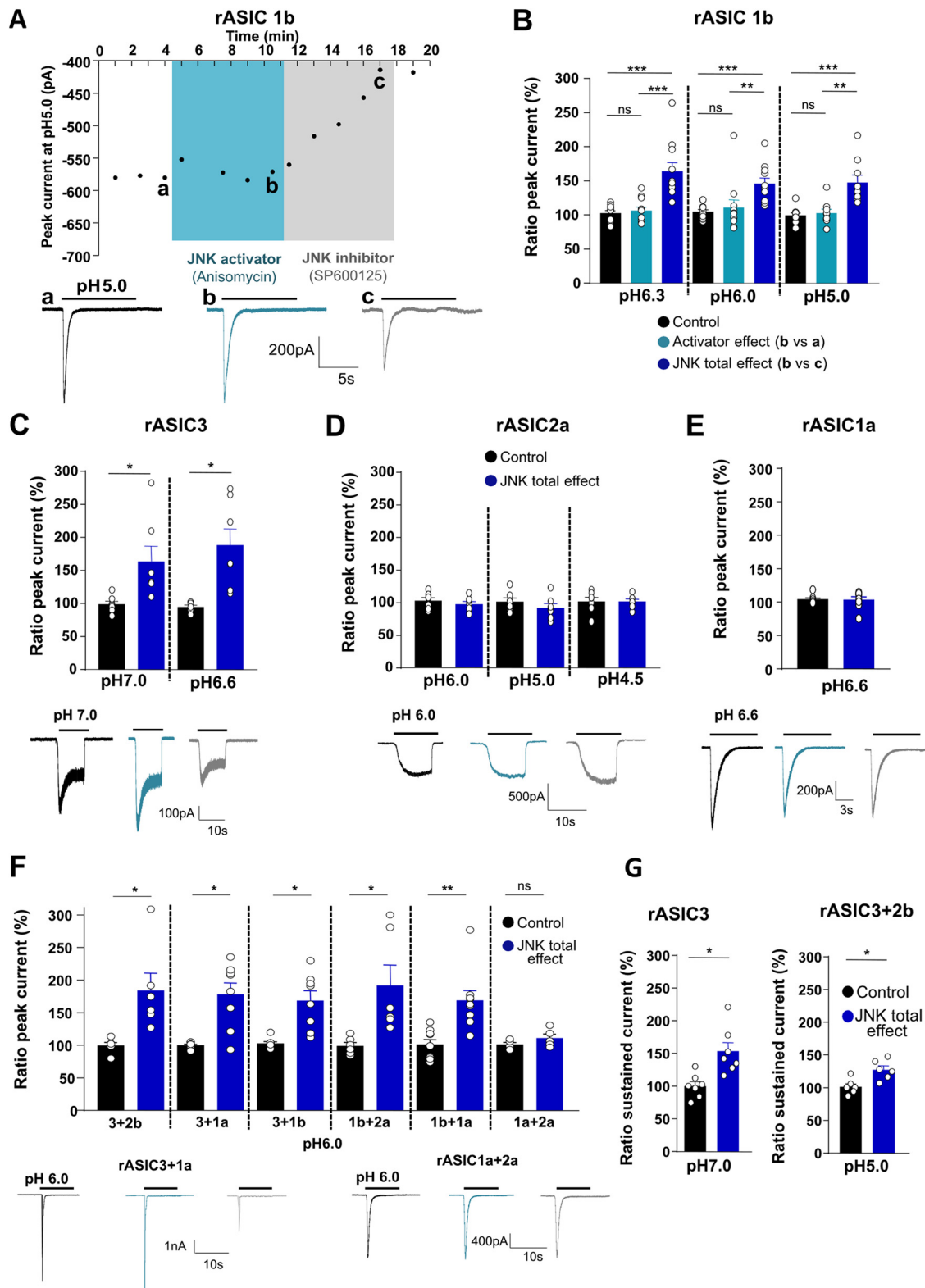
Figure 1. Regulation of recombinant rodent ASIC peak currents by JNK. **A**, Top, Representative time course of whole-cell rASIC1b current peak amplitude recorded at −60 mV in HEK293 cells. Currents were activated by a pH drop from 7.4 to 5.0. Anisomycin (50 μM) and the JNK inhibitor SP600125 (50 μM) were successively applied in the extracellular solution. Bottom, Representative current traces of rASIC1b current in control condition (a, black), after anisomycin application (b, cyan) and after SP600125 application (c, gray). **B**, Potentiation by JNK of rASIC1b current. Ratio (%) of amplitude of H^+-activated rASIC1b peak current activated at different pHs (conditioning pH 7.4), in the three pharmacological conditions shown in **A**. Individual data points and mean ± SEM are shown ($n = 9$–11 cells). Control (black) values were calculated from the ratio of the last two control currents, activator effects (cyan) were calculated from the ratio of b/a current amplitudes, and the total JNK effects (blue) were calculated from the ratio of b/c, that is, the ratio between the current amplitude after anisomycin and the maximally inhibited current amplitude after SP600125 perfusion. One-way ANOVA ($F_{(2,20)} = 26.50$, $p < 0.0001$, followed by Tukey's *post hoc* test, ***$p < 0.0001$, pH 6.3, JNK total effect vs control, ***$p < 0.0001$ anisomycin vs JNK, ns (non significant), $p = 0.91$ anisomycin vs control; $F_{(2,20)} = 12.01$, $p = 0.0004$, ***$p = 0.0006$, pH 6.0, JNK total effect vs control, **$p = 0.0027$ anisomycin vs JNK, ns $p = 0.77$ anisomycin vs control; $F_{(2,16)} = 12.8$, $p = 0.0005$, ***$p = 0.0009$, pH 5.0, JNK total effect vs control, **$p = 0.0018$ anisomycin vs JNK, ns, $p = 0.92$ anisomycin vs control). **C–**

containing channels, respectively. The different pharmacological profiles of ASIC currents in neurons and the inferred ASIC channel subtypes possibly associated are listed in Table 2. Neurons expressing an ASIC-like current can be found in DRG neuron populations of both small and medium/large diameters (membrane capacitance <40 pF and >40 pF, respectively), regardless of the display of a prominent shoulder on the falling phase of the action potential (data not shown), a feature of nociceptive neurons (Petruska et al., 2000), consistent with the broad distribution of ASICs in the global sensory neuron population.

The MAPK activator anisomycin was then applied on mouse and rat ASIC-expressing neurons ($n = 40$ and 20, respectively) and showed little potentiating effect on the ASIC peak current associated with various pharmacological profiles (Fig. 5A–C, light blue bars), whereas subsequent perfusion of the JNK inhibitor SP600125 induced a marked reduction of the current amplitude below the control level, thus revealing a high basal level of regulation of ASIC currents by JNK in at least 80% of the neurons tested in mouse and rat (32/40 and 18/20 neurons, respectively; Table 2). The culture process used is indeed known to increase the basal activity of the JNK pathway (Kristiansen and Edvinsson, 2010). A total JNK effect of $+100.8 \pm 17.4\%$ at pH 5.0 ($p < 0.0001$) and $+107 \pm 19.0\%$ at pH 6.6 ($p < 0.0001$) in mouse DRG neurons, and of $+78.8 \pm 13.6\%$ at pH 5.0 ($p = 0.0002$) and $+66.6 \pm 15.5\%$ at pH 6.6 ($p = 0.0001$) in rat DRG neurons was calculated (Fig. 5B–C, dark blue bars). Interestingly, a small subset of mouse neurons expressed APETx2-sensitive (i.e., ASIC3-containing) channels but JNK-insensitive currents (Table 2; Fig. 5D, upper traces), whereas all currents sensitive to APETx2 were sensitive to JNK in rat (Table 2; Fig. 5D, lower traces). This is consistent with the previous experiments in HEK293 cells (Figs. 1-4) and with the fact that the JNK regulation in mice solely involves the ASIC1b, but not the ASIC3, subunit. A large proportion of neurons expressing APETx2-sensitive currents in mice were, however, regulated by JNK (Table 2; Fig. 5A, lower traces), suggesting that they flow through heteromeric ASIC3-containing channels also including the JNK-sensitive ASIC1b subunit. Two rat neurons displaying currents sensitive to mambalgin-1 and
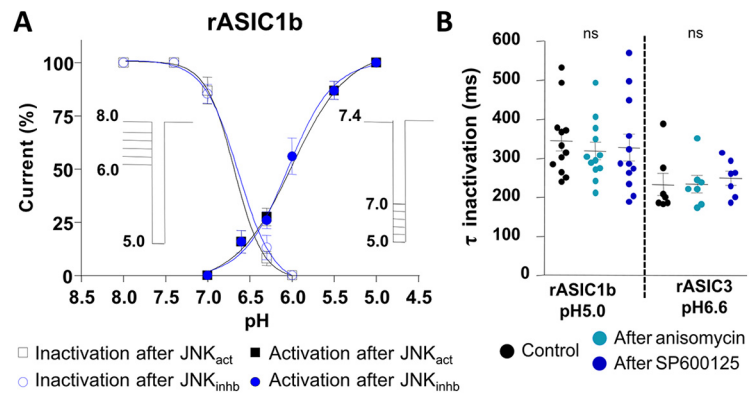
Figure 2. Effect of the JNK regulation on biophysical properties of rASIC1b and rASIC3 peak currents. **A**, The pH–dependent activation and inactivation curves of rat ASIC1b current after anisomycin (black) and SP600125 (blue) application on the same cells ($n = 4$–14). Inset, Protocols used for activation and inactivation. **B**, Scatter plots of inactivation time constants (in ms) of rASIC1b peak current activated at pH 5.0 and of rASIC3 peak current activated at pH 6.6 from a conditioning pH of 7.4, before and after extracellular perfusion with anisomycin (50 μM) and the JNK inhibitor SP600125 (50 μM). One-way ANOVA $F_{(2,33)} = 0.2172$, $p = 0.8059$, ns (non significant), ASIC1b, pH 5.0. One-way ANOVA $F_{(2,18)} = 0.1584$, $p = 0.8547$, ns, ASIC3, pH 6.6, $n = 7$–12 cells.

F, Potentiation by JNK of rASIC3 (**C**), rASIC2 (**D**), rASIC1a (**E**), and heteromeric (**F**; subunit combinations given below the bar graphs) currents. Ratio (%) of amplitude of H$^+$-activated ASIC peak current activated at different pHs (conditioning, pH 7.4). Mean potentiation by JNK (total effects) was calculated as in **B**. $n = 5$–9 cells for each channel subtype. Wilcoxon paired test versus control, rASIC3 *$p = 0.015$, pH 7.0 and pH 6.6, peak current; rASIC2a, ns (non significant), $p = 0.5781$, pH 6.0, $p = 0.4688$, pH 5.0, $p = 0.9375$, pH 4.5; rASIC1a, ns, $p = 0.7422$; rASIC3 + 2b, *$p = 0.0313$, pH 6.0; rASIC3 + 1a, *$p = 0.0156$, pH 6.0; rASIC3 + 1b, *$p = 0.0156$, pH 6.0; rASIC1b + 2a, *$p = 0.0313$, pH 6.0; rASIC1b + 1a, *$p = 0.039$, pH 6.0; rASIC1a + 2a, ns, $p = 0.437$, pH 6.0. Bottom (**C–E**), Representative current traces recorded at −60mV in control condition (black), and after anisomycin and SP600125 application (cyan and gray, respectively). **G**, JNK-Dependent potentiating effect on rASIC3 sustained window current activated at pH 7.0 (left) and on rASIC3 + 2b, pH 5.0-evoked sustained current (right). Conditioning pH 7.4, Wilcoxon paired test versus appropriate control, rASIC3, pH 7.0, *$p = 0.0156$; rASIC3 + 2b, *$p = 0.0313$; $n = 6$–7. JNK effect calculated and plotted as in Figure 1B.

PcTx1, likely expressing a majority of ASIC1a channels, were not sensitive to JNK (Table 2; Fig. 5D, middle-down traces), but mouse and rat neurons displaying currents sensitive to mambalgin-1 but not to PcTx1, likely expressing ASIC1b-containing channels, all showed JNK-regulated currents (Table 2; Fig. 5D, middle-up traces; Fig. 5A, lower traces), which is in good agreement with our previous experiments on recombinant ASIC channels in HEK293 cells.

Together, these data show that the activity of native ASIC1b- and ASIC3-containing channels is positively regulated by short-term JNK activation in most mouse and rat DRG neurons.
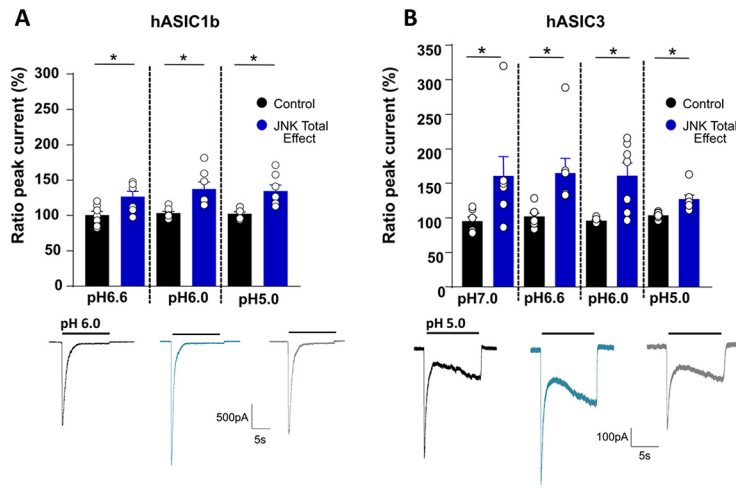
JNK-dependent upregulation of native ASIC currents in DRG neurons by the proinflammatory cytokine TNFα

The ability of endogenous pain-related mediators to regulate native ASIC channels in DRG neurons via the JNK pathway was then tested. The effect of TNFα, a pain-related cytokine and a well-known activator of receptor-mediated JNK activity (Natoli et al., 1997), was tested in acutely dissociated mouse DRG neurons (3–10 h in culture) deprived of neurotrophic factors to limit basal activation of JNK. The ASIC-like peak currents were characterized in these neurons as previously described and displayed pharmacological profiles close to those established in primary cultures (Fig. 6B vs Fig. 5B, pie charts). The subsequent perfusion of TNFα (10 ng/ml) on these neurons led to a rapid (within 5 min) increase of the ASIC peak current amplitude in more than half of the neurons tested (11/19; Fig. 6A,B; Table 2). Subsequent perfusion of the JNK inhibitor SP600125 induced a decrease of the current amplitude in 9/11 TNFα-responding neurons, including eight neurons that are only sensitive to mambalgin-1 and not to PcTx1, that is, likely expressing ASIC1b-containing channels (Table 2). There was no major difference in the magnitude of the increase induced by TNFα (TNFα effect compared with control) and the TNFα-JNK total effect ($+36.4 \pm 11.1\%$ vs $+58.1 \pm 11.8\%$ at pH 5.0, and $+57.2 \pm 18.4$ vs $+62.3 \pm 15.8$ at pH 6.6, not statistically significantly different; Fig. 6B), showing no significant basal activation of the JNK pathway in the absence of neurotrophic factors. The TNFα-induced increase of the ASIC peak current amplitude therefore mainly involved activation of the JNK pathway. However, the potentiating effect of TNFα was not reversed by SP600125 in two of 11 neurons,

Figure 3. JNK regulation of human ASIC1b and ASIC3 peak currents. **A,B**, Top, Potentiation by JNK (total effects) of recombinant H$^+$-activated human ASIC1b (hASIC1b, **A**) and ASIC3 (hASIC3, **B**) peak currents expressed in HEK293 cells, activated at different pHs (conditioning pH 7.4) and recorded at −60mV (calculated and plotted as in Figure 1B). $n = 7$ cells for each channel subtype. Wilcoxon paired test versus control, hASIC1b, *p= 0.0469, pH 6.6, p = 0.0313, pH 6.0, p = 0.0156, pH 5.0; hASIC3, *p = 0.0156, pH 7.0, p = 0.0156, pH 6.6, p = 0.0156, pH 6.0, p = 0.0156, pH 5.0. Bottom, Representative current traces in control condition (black), and after anisomycin (cyan) or SP600125 (gray) application.
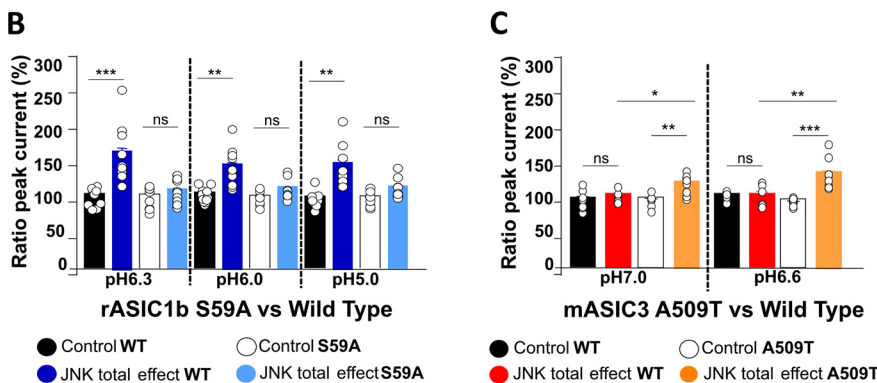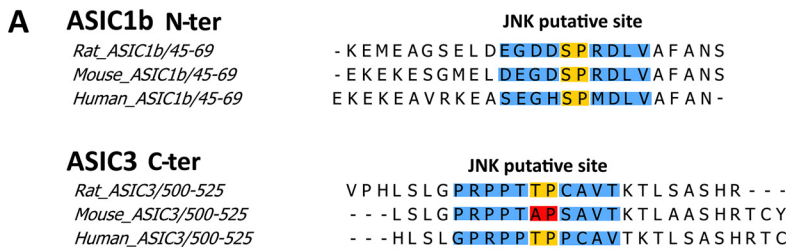
Figure 4. The JNK regulation is species dependent and depends on a putative phosphorylation site within the intracellular domains of ASIC1b and ASIC3 subunits. **A**, Partial sequence alignments of rat, mouse, and human ASIC1b and ASIC3 intracellular N- and C-terminal domains, respectively. The potential JNK phosphorylation sites found with GPS and ELM software are highlighted (phosphorylated S/T residues followed by P). **B,C**, Potentiation by JNK (total effects) of H$^+$-activated rASIC1b WT and S59A mutant currents (**B**) and of H$^+$-activated mASIC3 WT and A509T mutant currents (**C**), recorded at different pHs (calculated and plotted as in Figure 1B). **B**, one-way ANOVA followed by Tukey's *post hoc* test: $F_{(3,36)} = 14.45$, $p < 0.0001$, ns (non significant), $p = 0.9067$, rASIC1bS59A, pH 6.3, control versus JNK, ***$p < 0.0001$, rASIC1b WT, pH 6.3, control versus JNK; $F_{(3,36)} = 14.10$, $p < 0.0001$, ns, $p = 0.4476$, rASIC1bS59A, pH 6.0, control versus JNK, ***$p < 0.0001$, rASIC1b WT, pH 6.0, control versus JNK, $F_{(3,34)} = 12.89$, $p < 0.0001$, ns, $p = 0.3334$, rASIC1bS59A, pH 5.0, control versus JNK, ***$p < 0.0001$, rASIC1b WT, pH 5.0, control versus JNK, $n = 9$–12 cells. **C**, One-way ANOVA followed by Tukey's *post hoc* test: $F_{(3,28)} = 8.09$, $p = 0.0005$, ns, $p = 0.8014$, mASIC3 WT, pH 7.0, control versus JNK, **$p = 0.0011$, mASIC3A509T, pH 7.0, control versus JNK, *$p = 0.0198$, mASIC3A509T, pH 7.0, JNK versus mASIC3 WT, JNK. $F_{(3,27)} = 11.88$, $p < 0.0001$, ns, $p > 0.9999$, mASIC3 WT, pH 6.6, control versus JNK, ***$p < 0.0001$, mASIC3A509T, pH 6.6, control versus JNK, **$p = 0.0027$, mASIC3A509T, pH 6.6, JNK versus mASIC3 WT JNK, $n = 6$–9 cells.

including a neuron that predominantly expressed ASIC1b-containing channels (i.e., sensitive to mambalgin-1 and not to PcTx1; Table 2), suggesting a possible minor involvement of other JNK-independent TNFα-associated regulations of ASICs in DRG neurons.

The proinflammatory cytokine TNFα therefore appears to be a fast and potent upregulator of ASIC1b-containing channel activity in mouse sensory neurons, mainly through the activation of the JNK pathway.

Potentiation by JNK of the acid-induced cutaneous pain in inflammatory conditions in mice and the implication of peripheral ASIC1-containing channels

The physiopathological relevance of JNK regulation of ASIC channels was tested *in vivo* on the spontaneous pain behavior induced by subcutaneous i.pl. injection of a pH 5.0 solution in the mouse hindpaw. The lack of regulation of mouse ASIC3 subunit was a good opportunity to investigate *in vivo* the specific role of the JNK regulation of ASIC1b-containing channels. A pharmacological approach has been used where compounds (or corresponding vehicles) were preinjected 10 min before their coinjection with the pH 5.0 solution. In naive mice, a pH 5.0 i.pl. injection (preceded by preinjection of vehicle) induced a very small behavioral response during the first 5 min interval (5.9 ± 1.2 s, $n = 26$; Fig. 7A, blue points). In the presence of anisomycin (500 μM), the acid-induced response was significantly increased (10.8 ± 2.9 s, $n = 23$, $p = 0.0120$, red points), and was also stronger than the effect of anisomycin alone (6.3 ± 2.3 s, $n = 23$, $p = 0.0284$; Fig. 7A, orange points). Although these results already show some potentiation by anisomycin of the pH 5.0-induced pain in naive animals, the small amplitude of the effects precluded further investigation in these conditions.

A possible potentiation of acid-induced cutaneous pain by JNK was also tested in inflammatory conditions after an i.pl. injection of carrageenan in the hindpaw 3 h before testing the acid pH 5.0-induced spontaneous pain. The pH 5.0 injection induced a 10.7 ± 3.6 s ($n = 25$) mean response during the first 5 min interval (Fig. 7B, black points), with 76% of the tested mice showing a response longer than 3 s compared with only 14% of naive mice, thus showing that the local hindpaw inflammation not only increased the duration of the response but, above all, the number of responding mice. Anisomycin

Table 2. Pharmacological profiles of DRG-expressed JNK-sensitive and JNK-insensitive ASIC currents and their possible association with ASIC channel subtypes inferred from peptide toxin blocking selectivity

Toxin inhibition profiles (i.e., DRG currents only inhibited by the indicated toxins among the three tested)	Number of neurons expressing toxin-inhibited ASIC currents[a]			Possibly associated ASIC channel subtypes[b] (based on the pharmacological profiles shown in Table 1)			
	Mouse (JNK-sensitive/total) (32/40)	Rat (JNK-sensitive/total) (18/20)	Mouse TNFα (TNFα-sensitive/JNK-sensitive/total) (11/9/19)				
Mamb-1 + APETx2 + PcTx1	**5**/9	**6**/6	2/**1**/7	ASIC1a	ASIC1a/2a or **ASIC1b-containing**	**ASIC3-containing**	
Mamb-1 + APETx2	**17**/21	**5**/5	6/**6**/7		ASIC1a/2a or **ASIC1b-containing**	**ASIC3-containing**	
Mamb-1 + PcTx1		**3**/5		ASIC1a	ASIC1a/2a or **ASIC1b-containing**		
Mamb-1	**10**/10		3/**2**/5		ASIC1a/2a or **ASIC1b-containing**		
APETx2		**4**/4					**ASIC3-containing**

[a] Number of sensory neurons expressing toxin-inhibited ASIC currents in mouse and rat DRG primary cultures, and in TNFα-treated, acutely dissociated mouse DRG neurons, and their distribution according to the different pharmacological profiles determined by testing the inhibitory effects of mambalgin-1 (1 μM), APETx2 (3 μM), and PcTx1 (20 nM). Numbers of neurons expressing ASIC currents regulated by JNK are indicated in bold.
[b] ASIC channel subtypes possibly associated with the different pharmacological profiles based on data shown in Table 1. Channel subtypes regulated by JNK in vitro are indicated in bold.

Table 3. Main electrophysiological properties of rat and mouse sensory neurons obtained from primary cultures

Culture type	Capacitance (pF)	Resting membrane potential (mV)	Action potential duration (ms)	Rheobase (pA)	Transient current density (pA/pF, pH 5.0)	Peak current inactivation time constant (ms, pH 5.0)
Mouse DRG	42.81 ± 2.01 (15.00/94.00)	−58.79 ± 0.53 (−71.00/−40.00)	3.03 ± 0.18 (0.84/8.37)	604.80 ± 47.57 (50.00/2611.00)	35.02 ± 4.03 (2.12/119.40)	376.20 ± 50.20 (73.00/1472.00)
Rat DRG	42.25 ± 2.72 (18.00/89.00)	−57.59 ± 1.11 (−76.00/−40.00)	4.87 ± 0.35*** (1.09/10.03)	1446.00 ± 147.40*** (50.00/4950.00)	85.13 ± 18.16** (3.29/342.30)	562.30 ± 89.72* (159.00/1436.00)

Mean ± SEM (minimum/maximum), n = 15–101 neurons from 4–10 independent cultures (1–4 d in culture, same culture conditions). Mann–Whitney test to compare properties of recorded mouse DRG neurons versus properties of recorded rat DRG neurons for each category: capacitance, ns (non significant), p = 0.8222, resting membrane potential, ns, p = 0.2400, action potential duration ***p < 0.0001, rheobase ***p < 0.0001, current density **p = 0.005, inactivation time constant *p = 0.0157.

induced a significantly enhanced pH 5.0-induced pain behavior during the first 5 min (35.7 ± 6.8 s, n = 25; Fig. 7B, red points) compared with the effect of vehicle (10.1 ± 2.3 s, n = 26, p < 0.001; Fig. 7B, blue points) or with the effect of anisomycin alone (9.3 ± 2.1 s, p < 0.001, n = 25; Fig. 7B, orange points). The potentiating effect of anisomycin on acidic pain was reversed by the JNK inhibitor SP600125 (500 μM), leading to a behavioral response of 12.1 ± 2.4 s (n = 25, p < 0.001; Fig. 7B, green points) that was similar to the response in the absence of anisomycin. JNK has therefore a major contribution to the anisomycin-induced acidic pain potentiation in inflammatory conditions. The response was significantly reduced in the presence of mambalgin-1 (34 μM), the specific ASIC1-containing channel inhibitor (Fig. 7C, pink points), to 20.8 ± 3.5 s (n = 23) during the first 5 min, compared with 32.0 ± 5.7 s (n = 25, p = 0.0196) in the presence of the corresponding vehicle (35% inhibition; Fig. 7C, red points). Coapplication of 10 μM APETx2, which inhibits ASIC3-containing channels, with mambalgin-1 (Fig. 7C, dark green points) did not produce further inhibition (20.7 ± 3.4 s, n = 23, p = 0.0180) compared with mambalgin-1 alone, supporting the ASIC3-independent nature of the JNK-potentiated acidic pain response that remains. The TRPV1 inhibitor capsazepine (CPZ, 10 μM) did not significantly inhibit the spontaneous pain response induced by i.pl. injection of pH 5.0 + anisomycin in an inflamed hindpaw (Fig. 7B, brown points), despite a tendency to slightly reduce the response (from 35.7 ± 6.8 s (n = 25) to 28.3 ± 6.8 s (n = 26), 5 min after injection), suggesting only a minor contribution of TRPV1 to JNK-stimulated, pH 5.0-triggered pain in inflammatory conditions.

These data show that ASIC1-containing channels are involved in the JNK-potentiated, acid-induced cutaneous pain in inflammatory conditions in mice.

Discussion

By combining electrophysiological approaches with specific pharmacologic tools, we identified a new JNK-mediated fast potentiation of the activity of ASIC1b- and ASIC3-containing channels. This regulation may involve a direct phosphorylation of the intracellular domains of the ASIC subunits as (1) it is disrupted by mutation of a putative JNK phosphorylation site in the ASIC1b N-terminal domain (S59A) and (2) it is absent in mouse ASIC3, which is naturally lacking the phosphorylation site because of the presence of an alanine (A509) instead of a threonine, but can be acquired by introducing a point mutation (A509T) recreating a JNK phosphorylation site. Native ASIC channels in DRG neurons are potentiated by JNK with a functional profile consistent with the data found from recombinant channels in HEK293 cells, and this JNK signaling pathway is involved in the fast potentiation of native ASIC currents by the proinflammatory cytokine TNFα in sensory neurons. Finally, ASIC1-containing channels contribute to the JNK potentiating effect on cutaneous acid-triggered pain in inflammatory conditions in mice.

MAPKs as potent post-translational regulators of ASIC channels

Our data support a role for JNK in the post-translational regulation of ASIC channels. We have combined in our protocols an activator (anisomycin) and an inhibitor (SP600125), which show at the concentration used (50 μM) good selectivity for JNK versus the other MAPKs (Bain et al., 2007). In addition, the ASIC current potentiation strictly depends on putative JNK phosphorylation sites in ASIC1b and ASIC3 subunits. Even if SP600125 has the potency to inhibit to some extent other kinases (like DYRK, PDK1, CK2, or SGK1; Bain et al., 2007), the predictive phosphorylation sites for these kinases present in the ASIC1b and/or ASIC3 intracellular domains are clearly different from the two that have been shown to be mandatory for the effect described here. In addition, some of these predictive phosphorylation sites such as SGK1 are also present in the ASIC1a or ASIC2a subunits, which are not affected by SP600125. A role for JNK is therefore
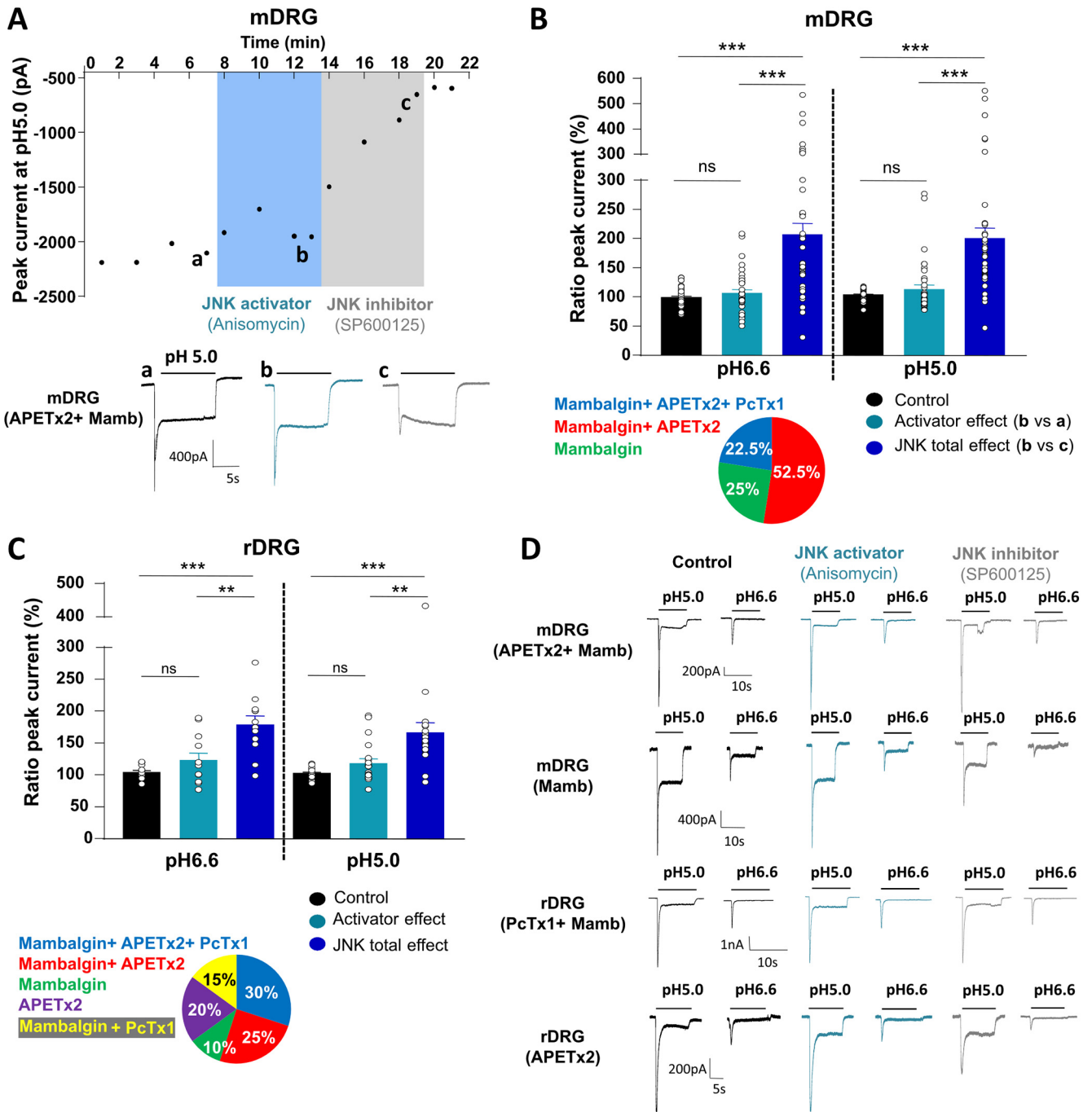
Figure 5. JNK regulates native ASIC peak currents in cultured rodent DRG neurons. ***A***, Top, Representative time course of mouse DRG (mDRG) neuron ASIC peak current amplitude recorded at −80 mV on stimulation by a shift from resting pH 7.4 to pH 5.0, and extracellular perfusion with anisomycin (50 μM) and the JNK inhibitor SP600125 (50 μM). Bottom, Representative current traces of APETx2 and mambalgin-1-sensitive currents (Tables 1, 2 for details). ***B***, Potentiation by JNK of H$^+$-activated mouse DRG (mDRG) neuron ASIC peak current recorded at different pHs (calculated and plotted as in Figure 1*B*), n = 36–40. One-way ANOVA followed by Tukey's *post hoc* test: $F_{(2,70)}$ = 27.68 p < 0.0001, ***p < 0.0001 control versus JNK pH 6.6, p < 0.0001 JNK versus anisomycin pH 6.6, ns (non significant) p = 0.6476 control versus anisomycin pH 6.6; $F_{(2,78)}$ = 22.04 p < 0.0001, ***p < 0.0001 control versus JNK pH 5.0, p < 0.0001 JNK versus anisomycin pH 5.0, ns p = 0.5620 control versus anisomycin pH 5.0. Bottom, Pie chart showing the proportion of ASIC peak currents with different pharmacological profiles tested for JNK regulation in mouse DRG neurons (n = 40) and determined by the effects of the three ASIC inhibitory toxins mambalgin-1 (1 μM), APETx2 (3 μM) and PcTx1 (20 nM). A 20% threshold for inhibition has been used (Tables 1, 2). ***C***, Potentiation by JNK of H$^+$-activated rat DRG (rDRG) neuron ASIC peak current recorded at different pHs (same protocol as in ***B***), n = 12–20. One-way ANOVA followed by Tukey's *post hoc* test: $F_{(2,22)}$ = 13.96, p = 0.0002, ***p = 0.0001 control versus JNK pH 6.6, **p = 0.0026 JNK versus anisomycin pH 6.6, ns p = 0.4331 control versus anisomycin pH 6.6; $F_{(2,38)}$ = 10.62, p = 0.0002, ***p = 0.0002 control versus JNK pH 5.0, ***p = 0.0038 JNK versus anisomycin pH 5.0, ns, p = 0.2877 control versus anisomycin pH 5.0. Bottom, Pharmacological profiles (determined as in ***B***; Tables 1, 2 for interpretations) of the ASIC peak currents in rat DRG neurons tested for JNK regulation (n = 20). ***D***, Representative current traces of rat and mouse DRG neuron ASIC currents with different pharmacological profiles regarding inhibition by mambalgin-1 (Mamb), PcTx1, and APETx2 in control condition (black), and after anisomycin and SP600125 application (cyan and gray, respectively). The toxins inhibiting the current by at least 20% were indicated in brackets. Currents were recorded at −80mV and activated at two different pHs (Tables 1, 2). The same culture conditions were used for rat and mouse DRG neurons.

strongly supported by these complementary elements, even if minor contributions of other signaling pathways cannot be completely excluded.

A large range of mediators of various origins have been shown to directly or indirectly modulate the activity of ASIC channels. Several pain-related signaling pathways targeting ASICs have been previously characterized, including PKC (Baron et al., 2002), PKA (Leonard et al., 2003), or phosphoinositide 3-kinase (PI3K)-protein kinase B (PKB/Akt; Duan et al., 2012). A MAPK-dependent transcriptional regulation of ASIC3 has been involved in the effect of NGF (Mamet et al., 2003; Chaumette et al., 2020) or interleukin 1β (Ross et al., 2016), and a MAPK-dependent transcriptional regulation of ASIC1a has also been associated with the effect of interleukin 6 (Zhou et al., 2015) or oxidative stress (Wu et al., 2021), but a MAPK-dependent phosphorylation of ASIC channels has never been described so far. Our data are consistent with a phosphorylation by JNK of the ASIC1b and ASIC3 (except mouse ASIC3) subunits. The time scale of the effect (<10 min) makes an indirect transcriptional contribution to the effect unlikely. JNK may therefore participate in nociceptive neurons in the generation of pain hypersensitivity through transcription-independent, direct phosphorylation of ion channels in addition to its well-known transcription-dependent modulation of pain-related genes. The biophysical properties of ASIC1b channels including gating, proton sensitivity, inactivation time constant, and conductance are not affected by the JNK regulation, which may suggest an increase in the opening probability of the channel or an effect mediated at least in part through an increase in channel trafficking to the plasma membrane. Enhanced forward trafficking and increased surface expression of ASICs via direct phosphorylation has been already reported for the regulation of ASIC1a by BDNF through the PI3K/Akt pathway in the spinal cord (Duan et al., 2012). The effect of JNK phosphorylation on a given target is often linked to the establishment of new protein–protein interactions (Zeke et al., 2016). This phosphorylation could therefore be a switch to increase the channel number at the plasma membrane, as shown previously (Simonetti et al., 2014), or to prevent ion channels from being internalized.
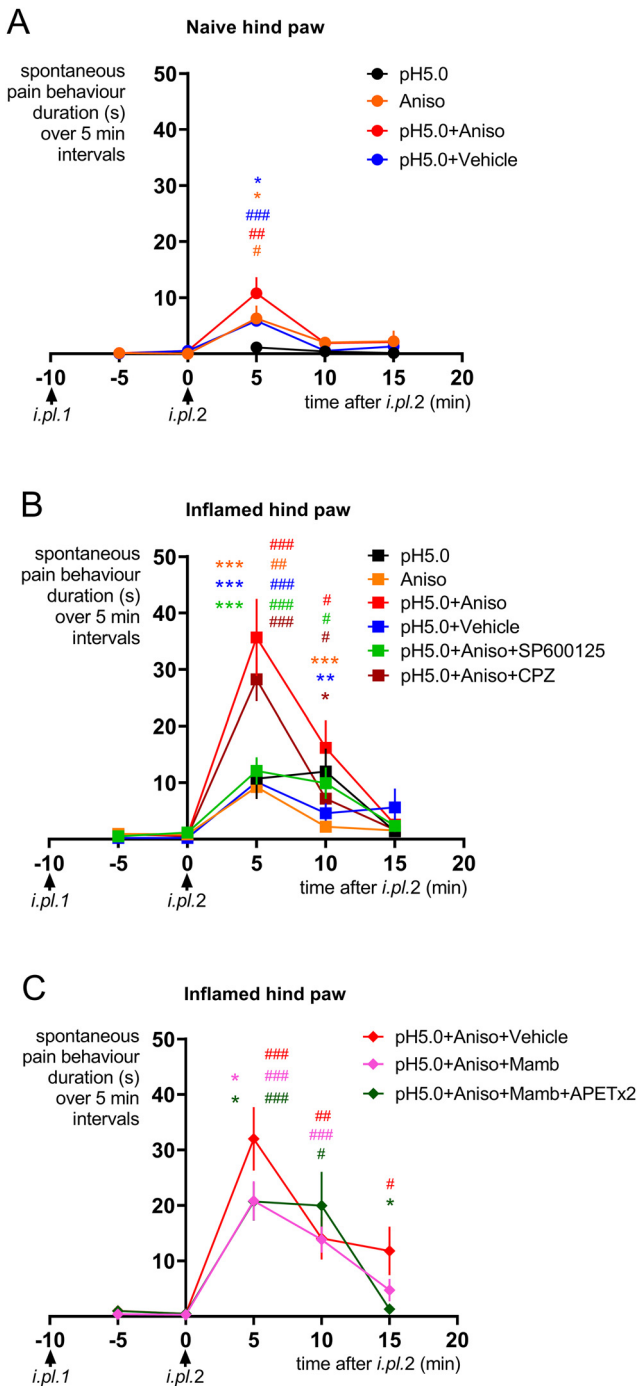
Native proton-gated currents of sensory neurons are strongly potentiated by JNK to modulate pain sensing

Our results demonstrate that the vast majority of DRG neurons expressing ASIC currents (including small and medium/large neurons) are positively regulated by JNK signaling. The molecular identity of these currents can be, at least partially, inferred from their biophysical properties and their sensitivity to different ASIC toxins specifically blocking a complementary set of homomeric and/or heteromeric channels (Baron et al., 2013). Some JNK-insensitive currents have been only recorded in ASIC1a-expressing neurons in rats, or in ASIC3-expressing neurons in mice (All ASIC3-expressing neurons display JNK-regulated ASIC currents in rats). It fits with our experiments on
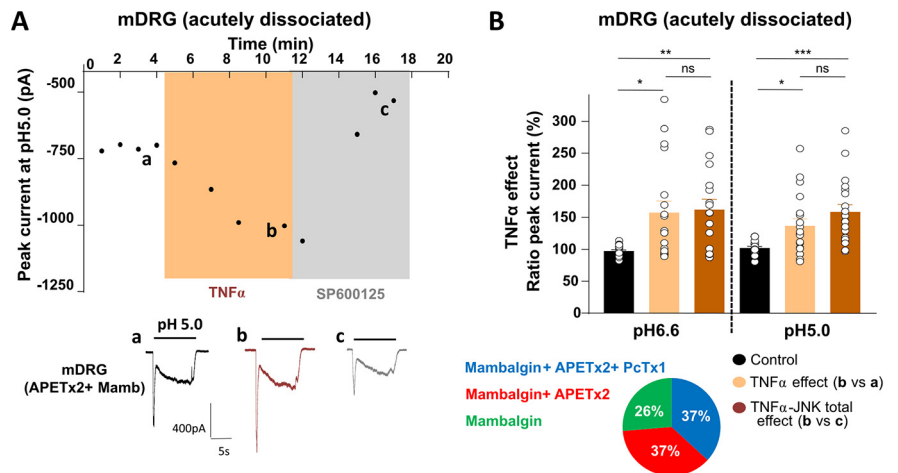
Figure 6. TNFα potentiates H$^+$-activated ASIC peak currents from acutely dissociated mouse sensory neurons through JNK activation. **A**, Top, Representative time course of mouse DRG (mDRG) ASIC peak current amplitude on stimulation at pH 5.0 from conditioning pH 7.4 and extracellular perfusion with TNFα (10 ng/ml) and the JNK inhibitor SP600125 (50 μM). Bottom, Representative pH 5.0-evoked mambalgin-1- (Mamb) and APETx2-sensitive current traces (Tables 1, 2). **B**, Mean potentiation by TNFα of H$^+$-activated ASIC peak currents in mDRG neurons recorded at different pHs (ratio b/a, plotted as in Figure 1B) and comparison with the TNFα-JNK total effect (ratio b/c). n = 18–19, one-way ANOVA followed by Tukey's *post hoc* test: $F_{(2,34)} = 6.461$, $p = 0.0042$, **$p = 0.0075$ control versus TNF-JNK, pH 6.6, *$p = 0.0143$, control versus TNF, pH 6.6, ns (non significant), $p = 0.4331$, TNF versus TNF-JNK, pH 6.6; $F_{(2,36)} = 10.47$, $p = 0.0003$, ***$p = 0.0002$, control versus TNF-JNK, pH 5.0, *$p = 0.0224$, control versus TNF, pH 5.0, ns, $p = 0.2014$, TNF versus TNF-JNK, pH 5.0. Bottom, Pharmacological profiles of the ASIC peak currents in mouse DRG neurons tested for TNFα regulation (as determined in Figure 4B; n = 19).

recombinant channels in HEK293 cells showing a regulation supported by both the ASIC1b and ASIC3 subunits in rats but only the ASIC1b subunit in mice. However, >70% of mouse ASIC3-expressing neurons display JNK-regulated currents despite the lack of regulation of the ASIC3 subunit, suggesting the presence in DRG neurons of our primary cultures of a high proportion of ASIC3 heteromeric channels also containing ASIC1b. Multiplexed *in situ* hybridization has confirmed a significant colocalization of ASIC1b and ASIC3 transcripts in mouse DRG neurons (Chang et al., 2019; Papalampropoulou-Tsiridou et al., 2020). It further supports, together with the high proportion of JNK-regulated ASIC1b-expressing neurons in mice, a broad functional expression of ASIC1b in sensory neurons. This is fully consistent with our previous work indicating a significant role for ASIC1b-containing channels in pain (Diochot et al., 2012, 2016). A possibly more robust response could be expected in rats from the regulation by JNK of both ASIC1b- and ASIC3-containing channels. However, the functional involvement in DRG neurons of a high proportion of ASIC3 heteromeric channels also containing ASIC1b supports the possibility of a significant overlap (at least in our culture conditions) between the ASIC1b- and ASIC3-dependent JNK regulations when they are both present like in rats and humans. Our *in vivo* experiments in mice based on local application of specific ASIC blockers, further support the involvement of peripheral ASIC1-containing channels, most probably ASIC1b-containing channels regarding the *in vitro* data on recombinant and native ASICs, in the JNK-potentiated acidic pain in inflammatory conditions. Interestingly, the strong potentiating effect observed in inflammatory conditions is consistent with a role for ASIC1b in producing hyperalgesic priming, a process that has been proposed to be involved in the transition from acute to chronic pain, as recently suggested in a preclinical model of muscle pain (Chang et al., 2019). The effect was, however, only partially inhibited by the specific ASIC blockers, suggesting the involvement, at least in our conditions in mice, of other JNK-

regulated and ASIC-independent processes, with minor, if any, contribution of TRPV1 channels.

Direct regulation of DRG-specific ASIC1b- and ASIC3-containing channels by JNK represents a new mechanism for pathologic potentiation of ASIC channels on activation of this signaling pathway in peripheral sensory neurons. Extracellular mediators contributing to pain sensitization can participate in this process, like the cytokine TNFα (Zelenka et al., 2005), which rapidly increases the amplitude of ASIC currents in a MAPK-dependent manner as shown here and by Wei et al. (2021). However, a study reported a lack of potentiating effect of TNFα on the rat vagal sensory neuron rapid transient current mediated by ASICs but a significant increase of the slow sustained current mediated by TRPV1 through a cyclooxygenase 2-dependent mechanism (Hsu et al., 2017). Differences in the experimental conditions (origin of the neurons and culture conditions, TNFα concentration, perfusion time) could explain these different results. Interestingly, the JNK-dependent regulation of the activity of ASIC1b- and ASIC3-containing channels in sensory neurons is reminiscent of the one previously mentioned for BDNF, PI3K/Akt pathway, and ASIC1a channels in the spinal cord (Duan et al., 2012).

←

+ Anisomycin + vehicle (500 μM and 0.05% BSA, respectively, red symbols, n = 25), pH 5.0 + Anisomycin + Mamb-1 (500 μM and 34 μM, respectively, pink symbols, n = 23), pH 5.0 + Anisomycin + Mambalgin-1 + APETx2 (500 μM, 34 μM, and 10 μM respectively, dark green symbols, n = 23). Data are presented as mean ± SEM as a function of time. *A*, Data obtained with the double intraplantar protocol were compared with pH 5.0 + Anisomycin with a two-way ANOVA followed by Dunnett's *post hoc* test: time $F_{(4,276)}$ = 18.03, $p < 0.0001$, treatment $F_{(2,69)}$ = 1.520, $p = 0.2260$, time × treatment $F_{(8,276)}$ = 0.8958, $p = 0.5204$, *$p = 0.0284$ Aniso T = 5 min, *$p = 0.0120$, pH 5.0 + Vehicle T = 5 min, other data not significantly different (p values not given). To determine whether a pain response duration was significant, each point of the kinetics was compared with value during the 5 min interval before i.pl.2 injection with a two-way ANOVA followed by Dunnett's *post hoc* paired comparison on the same mice: time $F_{(2.460, 637.2)}$ = 106.7, $p < 0.0001$, treatment $F_{(10,259)}$ = 10.48, $p < 0.0001$, #$p = 0.0410$ Anisomycin T = 5 min, ##$p = 0.0076$, pH 5.0 + Aniso T = 5 min, ###$p = 0.0008$, pH 5.0 + Vehicle T = 5 min. *B*, Data obtained with the double intraplantar protocol were compared with pH 5.0 + Anisomycin with a two-way ANOVA followed by Dunnett's *post hoc* test: time $F_{(4.488)}$ = 57.52, $p < 0.0001$, treatment $F_{(4,122)}$ = 9.101, $p < 0.0001$, time × treatment $F_{(16,488)}$ = 5.911, $p < 0.0001$, Aniso T = 5 min, ***$p < 0.0001$, pH 5.0 + Vehicle T = 5 min, ***$p < 0.0001$, pH 5.0 + Anisomycin + SP600125 T = 5 min, ***$p < 0.0001$, ns, $p = 0.0789$, pH 5.0 + Anisomycin + CPZ T = 5 min, Aniso T = 10 min, ***$p = 0.0001$, pH 5.0 + Vehicle T = 10 min, ** $p = 0.0016$, pH 5.0 + Anisomycin + SP600125 T = 10 min, ns, $p = 0.1763$, * $p = 0.0215$, pH 5.0 + Anisomycin + CPZ T = 10 min, other data not significantly different for T = −10 min, T = −5 min, and T = 15 min (p values are not given). *C*, Data obtained with the double intraplantar protocol were compared with pH 5.0 + Anisomycin + Vehicle with a two-way ANOVA followed by Dunnett's *post hoc* test: time $F_{(4,272)}$ = 36.84, $p < 0.0001$, treatment $F_{(2,68)}$ = 1.836, $p = 0.1673$, time × treatment $F_{(8,272)}$ = 1.71, $p = 0.0851$, pH 5.0 + Anisomycin + Mamb T = 5 min, *$p = 0.0196$, pH 5.0 + Anisomycin + Mamb + APETx2 T = 5 min, *$p = 0.0180$, pH 5.0 + Anisomycin + Mamb + APETx2 T = 15 min, *$p = 0.0300$, other data not significantly different (p values are not given). To determine whether a pain response duration was significant, each point of the kinetics in *B* and *C* was compared with value during the 5 min interval before i.pl.2 injection with a two-way ANOVA followed by Dunnett's *post hoc* paired comparison on the same mice: time $F_{(2.460, 637.2)}$ = 106.7, $p < 0.0001$, treatment $F_{(10,259)}$ = 10.48, $p < 0.0001$, ###$p = 0.0031$, Aniso T = 5 min, ###$p = 0.0007$, pH 5.0 + Vehicle T = 5 min, ###$p = 0.0001$ pH 5.0 + Aniso T = 5 min, #$p = 0.0168$, pH 5.0 + Aniso T = 10 min, ###$p = 0.0009$, pH 5.0 + Aniso + SP600125 T = 5 min, #$p = 0.0275$, pH 5.0 + Aniso + SP600125 T = 10 min, ###$p < 0.0001$, pH 5.0 + Aniso + CPZ T = 5 min, # $p = 0.0138$, pH 5.0 + Aniso + CPZ T = 10 min, ###$p < 0.0001$, pH 5.0 + Aniso + Vehicle T = 5 min, ##$p = 0.0051$, pH 5.0 + Aniso + Vehicle T = 10 min, ###$p < 0.0001$, pH 5.0 + Aniso + Mamb T = 5 min, ###$p < 0.0001$, pH 5.0 + Aniso + Mamb T = 10 min, ###$p < 0.0001$, pH 5.0 + Aniso + Mamb + APETx2 T = 5 min, #$p = 0.0116$, pH 5.0 + Aniso + Mamb + APETx2 T = 10 min, p values are not given for the other nonsignificant comparisons.

Figure 7. ASIC1-containing channels contribute to the JNK-induced potentiation of cutaneous acid-triggered pain in mice. *A*, Kinetics of spontaneous pain behavior duration (s) measured over 5 min intervals in naive mice hindpaw. Single intraplantar injection of pH 5.0 (black symbols, n = 28) and double intraplantar injection with drugs being preinjected alone (i.pl.1) 10 min before coinjection with pH 5.0 (i.pl.2): Anisomycin alone (500 μM, Aniso, orange symbols, n = 23), pH 5.0 + vehicle (DMSO 0.5%, blue symbols, n = 26), pH 5.0 + Anisomycin (500 μM, red symbols, n = 23). *B*, Kinetics of spontaneous pain behavior duration (s) measured over 5 min intervals in mice with local hindpaw inflammation (carrageenan 2%, 3 h). Single intraplantar injection of pH 5.0 (black symbols, n = 25) and double intraplantar injection protocol as described in *A*: Anisomycin alone (500 μM, Aniso, orange symbols, n = 25), pH 5.0 + vehicle (DMSO 0.5%, blue symbols, n= 26), pH 5.0 + Anisomycin (500 μM, red symbols, n = 25), pH 5.0 + Anisomycin + SP600125 (500 μM each, green symbols, n = 25), pH 5.0 + Anisomycin + CPZ (500 μM and 10 μM, respectively, brown symbols, n = 26). Data are presented as mean ± SEM as a function of time. *C*, Kinetics of spontaneous pain behavior duration (s) measured over 5 min intervals in mice with local hindpaw inflammation (carrageenan 2%, 3 h). Double intraplantar injection protocol: pH 5.0

In conclusion, our results identify a novel mechanism of post-translational regulation of sensory neuron-expressed ASIC1b- and ASIC3-containing channels by JNK, probably via direct phosphorylation of the channels, suggesting that ion channels can be direct downstream effectors of JNK in nociceptors. Our *in vivo* results on cutaneous pain illustrate the important role this regulation may have in various pathophysiological pain conditions involving the JNK signaling pathway including inflammatory, neuropathic, and migraine pain where ASIC1b- and/or ASIC3-containing channels have been involved (Deval et al., 2008; Diochot et al., 2012, 2016; Yan et al., 2013; Verkest et al., 2018). In addition, we provide further evidence of a large functional expression of ASIC1b-containing channels in sensory neurons, supporting the emerging role in pain of this ASIC isoform. The JNK regulation is conserved in human ASIC1b and ASIC3 channels, and interfering with this regulation at the channel level might be of potential therapeutic benefit against pain.

References

Askwith CC, Cheng C, Ikuma M, Benson C, Price MP, Welsh MJ (2000) Neuropeptide FF and FMRFamide potentiate acid-evoked currents from sensory neurons and proton-gated DEG/ENaC channels. Neuron 26:133–141.

Bain J, Plater L, Elliott M, Shpiro N, Hastie CJ, McLauchlan H, Klevernic I, Arthur JSC, Alessi DR, Cohen P (2007) The selectivity of protein kinase inhibitors: a further update. Biochem J 408:297–315.

Baron A, Deval E, Salinas M, Lingueglia E, Voilley N, Lazdunski M (2002) Protein kinase C stimulates the acid-sensing ion channel ASIC2a via the PDZ domain-containing protein PICK1. J Biol Chem 277:50463–50468.

Baron A, Diochot S, Salinas M, Deval E, Noël J, Lingueglia E (2013) Venom toxins in the exploration of molecular, physiological and pathophysiological functions of acid-sensing ion channels. Toxicon 75:187–204.

Benson CJ, Xie J, Wemmie JA, Price MP, Henss JM, Welsh MJ, Snyder PM (2002) Heteromultimers of DEG/ENaC subunits form H+-gated channels in mouse sensory neurons. Proc Natl Acad Sci U S A 99:2338–2343.

Bohlen CJ, Chesler AT, Sharif-Naeini R, Medzihradszky KF, Zhou S, King D, Sánchez EE, Burlingame AL, Basbaum AI, Julius D (2011) A heteromeric Texas coral snake toxin targets acid-sensing ion channels to produce pain. Nature 479:410–414.

Cadiou H, Studer M, Jones NG, Smith ESJ, Ballard A, McMahon SB, McNaughton PA (2007) Modulation of acid-sensing ion channel activity by nitric oxide. J Neurosci 27:13251–13260.

Chang C-T, Fong SW, Lee C-H, Chuang Y-C, Lin S-H, Chen C-C (2019) Involvement of acid-sensing ion channel 1b in the development of acid-induced chronic muscle pain. Front Neurosci 13:1247.

Chaumette T, Delay L, Barbier J, Boudieu L, Aissouni Y, Meleine M, Lashermes A, Legha W, Antraigue S, Carvalho FA, Eschalier A, Ardid D, Moqrich A, Marchand F (2020) c-Jun/p38MAPK/ASIC3 pathways specifically activated by nerve growth factor through TrkA is crucial for mechanical allodynia development. Pain 161:1109–1123.

Deval E, Lingueglia E (2015) Acid-sensing ion channels and nociception in the peripheral and central nervous systems. Neuropharmacology 94:49–57.

Deval E, Noël J, Lay N, Alloui A, Diochot S, Friend V, Jodar M, Lazdunski M, Lingueglia E (2008) ASIC3, a sensor of acidic and primary inflammatory pain. EMBO J 27:3047–3055.

Dinkel H, Michael S, Weatheritt RJ, Davey NE, Van Roey K, Altenberg B, Toedt G, Uyar B, Seiler M, Budd A, Jödicke L, Dammert MA, Schroeter C, Hammer M, Schmidt T, Jehl P, McGuigan C, Dymecka M, Chica C, Luck K, et al. (2012) ELM–the database of eukaryotic linear motifs. Nucleic Acids Res 40:D242–D251.

Diochot S, Baron A, Rash LD, Deval E, Escoubas P, Scarzello S, Salinas M, Lazdunski M (2004) A new sea anemone peptide, APETx2, inhibits ASIC3, a major acid-sensitive channel in sensory neurons. EMBO J 23:1516–1525.

Diochot S, Baron A, Salinas M, Douguet D, Scarzello S, Dabert-Gay A-S, Debayle D, Friend V, Alloui A, Lazdunski M, Lingueglia E (2012) Black mamba venom peptides target acid-sensing ion channels to abolish pain. Nature 490:552–555.

Diochot S, Alloui A, Rodrigues P, Dauvois M, Friend V, Aissouni Y, Eschalier A, Lingueglia E, Baron A (2016) Analgesic effects of mambalgin peptide inhibitors of acid-sensing ion channels in inflammatory and neuropathic pain. Pain 157:552–559.

Duan B, Liu D-S, Huang Y, Zeng W-Z, Wang X, Yu H, Zhu MX, Chen Z-Y, Xu T-L (2012) PI3-kinase/Akt pathway-regulated membrane insertion of acid-sensing ion channel 1a underlies BDNF-induced pain hypersensitivity. J Neurosci 32:6351–6363.

Escoubas P, De Weille JR, Lecoq A, Diochot S, Waldmann R, Champigny G, Moinier D, Ménez A, Lazdunski M (2000) Isolation of a tarantula toxin specific for a class of proton-gated Na+ channels. J Biol Chem 275:25116–25121.

Francois A, Kerckhove N, Meleine M, Alloui A, Barrere C, Gelot A, Uebele VN, Renger JJ, Eschalier A, Ardid D, Bourinet E (2013) State-dependent properties of a new T-type calcium channel blocker enhance Ca(V)3.2 selectivity and support analgesic effects. Pain 154:283–293.

Hsu C-C, Lin YS, Lin R-L, Lee L-Y (2017) Immediate and delayed potentiating effects of tumor necrosis factor-α on TRPV1 sensitivity of rat vagal pulmonary sensory neurons. Am J Physiol Lung Cell Mol Physiol 313: L293–L304.

Huang D, Ren L, Qiu C-S, Liu P, Peterson J, Yanagawa Y, Cao Y-Q (2016) Characterization of a mouse model of headache. Pain 157:1744–1760.

Hucho T, Levine JD (2007) Signaling pathways in sensitization: toward a nociceptor cell biology. Neuron 55:365–376.

Kristiansen KA, Edvinsson L (2010) Neurogenic inflammation: a study of rat trigeminal ganglion. J Headache Pain 11:485–495.

Kwak JY, Jung JY, Hwang SW, Lee WT, Oh U (1998) A capsaicin-receptor antagonist, capsazepine, reduces inflammation-induced hyperalgesic responses in the rat: evidence for an endogenous capsaicin-like substance. Neuroscience 86:619–626.

Leffler A, Mönter B, Koltzenburg M (2006) The role of the capsaicin receptor TRPV1 and acid-sensing ion channels (ASICS) in proton sensitivity of subpopulations of primary nociceptive neurons in rats and mice. Neuroscience 139:699–709.

Leonard AS, Yermolaieva O, Hruska-Hageman A, Askwith CC, Price MP, Wemmie JA, Welsh MJ (2003) cAMP-dependent protein kinase phosphorylation of the acid-sensing ion channel-1 regulates its binding to the protein interacting with C-kinase-1. Proc Natl Acad Sci U S A 100:2029–2034.

Li W-G, Yu Y, Zhang Z-D, Cao H, Xu T-L (2010) ASIC3 channels integrate agmatine and multiple inflammatory signals through the nonproton ligand sensing domain. Mol Pain 6:88.

Mamet J, Lazdunski M, Voilley N (2003) How nerve growth factor drives physiological and inflammatory expressions of acid-sensing ion channel 3 in sensory neurons. J Biol Chem 278:48907–48913.

Marra S, Ferru-Clément R, Breuil V, Delaunay A, Christin M, Friend V, Sebille S, Cognard C, Ferreira T, Roux C, Euller-Ziegler L, Noel J, Lingueglia E, Deval E (2016) Non-acidic activation of pain-related acid-sensing ion channel 3 by lipids. EMBO J 35:414–428.

Natoli G, Costanzo A, Ianni A, Templeton DJ, Woodgett JR, Balsano C, Levrero M (1997) Activation of SAPK/JNK by TNF receptor 1 through a noncytotoxic TRAF2-dependent pathway. Science 275:200–203.

Obata K, Yamanaka H, Kobayashi K, Dai Y, Mizushima T, Katsura H, Fukuoka T, Tokunaga A, Noguchi K (2004) Role of mitogen-activated protein kinase activation in injured and intact primary afferent neurons for mechanical and heat hypersensitivity after spinal nerve ligation. J Neurosci 24:10211–10222.

Papalampropoulou-Tsiridou M, Labrecque S, Godin AG, De Koninck Y, Wang F (2020) Differential expression of acid-sensing ion channels in mouse primary afferents in naïve and injured conditions. Front Cell Neurosci 14:103.

Petho G, Reeh PW (2012) Sensory and signaling mechanisms of bradykinin, eicosanoids, platelet-activating factor, and nitric oxide in peripheral nociceptors. Physiol Rev 92:1699–1775.

Petruska JC, Napaporn J, Johnson RD, Gu JG, Cooper BY (2000) Subclassified acutely dissociated cells of rat DRG: histochemistry and patterns of capsaicin-, proton-, and ATP-activated currents. J Neurophysiol 84:2365–2379.

Ross JL, Queme LF, Cohen ER, Green KJ, Lu P, Shank AT, An S, Hudgins RC, Jankowski MP (2016) Muscle IL1β drives ischemic myalgia via ASIC3-mediated sensory neuron sensitization. J Neurosci 36:6857–6871.

Salinas M, Lazdunski M, Lingueglia E (2009) Structural elements for the generation of sustained currents by the acid pain sensor ASIC3. J Biol Chem 284:31851–31859.

Simonetti M, Agarwal N, Stösser S, Bali KK, Karaulanov E, Kamble R, Pospisilova B, Kurejova M, Birchmeier W, Niehrs C, Heppenstall P, Kuner R (2014) Wnt-Fzd signaling sensitizes peripheral sensory neurons via distinct noncanonical pathways. Neuron 83:104–121.

Smith ES, Cadiou H, McNaughton PA (2007) Arachidonic acid potentiates acid-sensing ion channels in rat sensory neurons by a direct action. Neuroscience 145:686–698.

Verkest C, Piquet E, Diochot S, Dauvois M, Lanteri-Minet M, Lingueglia E, Baron A (2018) Effects of systemic inhibitors of acid-sensing ion channels 1 (ASIC1) against acute and chronic mechanical allodynia in a rodent model of migraine. Br J Pharmacol 175:4154–4166.

Wei S, Qiu CY, Jin Y, Liu TT, Hu WP (2021) TNF-α acutely enhances acid-sensing ion channel currents in rat dorsal root ganglion neurons via a p38 MAPK pathway. J Neuroinflammation 18:92.

Wu B-M, Bargaineer J, Zhang L, Yang T, Xiong Z-G, Leng T-D (2021) Upregulation of acid sensing ion channel 1a (ASIC1a) by hydrogen peroxide through the JNK pathway. Acta Pharmacol Sin 42:1248–1255.

Xue Y, Ren J, Gao X, Jin C, Wen L, Yao X (2008) GPS 2.0, a tool to predict kinase-specific phosphorylation sites in hierarchy. Mol Cell Proteomics 7:1598–1608.

Yan J, Wei X, Bischoff C, Edelmayer RM, Dussor G (2013) pH-evoked dural afferent signaling is mediated by ASIC3 and is sensitized by mast cell mediators. Headache 53:1250–1261.

Zeke A, Misheva M, Reményi A, Bogoyevitch MA (2016) JNK Signaling: regulation and Functions Based on Complex Protein-Protein Partnerships. Microbiol Mol Biol Rev 80:793–835.

Zelenka M, Schäfers M, Sommer C (2005) Intraneural injection of interleukin-1beta and tumor necrosis factor-alpha into rat sciatic nerve at physiological doses induces signs of neuropathic pain. Pain 116:257–263.

Zhou R, Wu X, Wang Z, Ge J, Chen F (2015) Interleukin-6 enhances acid-induced apoptosis via upregulating acid-sensing ion channel 1a expression and function in rat articular chondrocytes. Int Immunopharmacol 29:748–760.